Biochimica et Biophysica Acta, 1024 (1990) 139–151
Elsevier

BBAMEM 74838

Statistical thermodynamics of association colloids. IV. Inhomogeneous membrane systems

Frans A.M. Leermakers, Jan M.H.M. Scheutjens and Johannes Lyklema

Laboratory for Physical and Colloid Chemistry, Wageningen Agricultural University, Wageningen (The Netherlands)

(Received 12 September 1989)
(Revised manuscript received 19 January 1990)

Key words: Membrane–protein interaction; Lattice model; Self-consistent field; Boundary lipid; Protein channel; Nonmixing lipid; Lateral phase separation

A previously developed self-consistent field theory to describe the equilibrium properties of lipid-like membranes is extended to allow the presence of inhomogeneities parallel to the membrane. Conformations of lipid molecules and foreign ('guest') molecules in the membrane are obtained by step-weighted random walk generation of the chains on a lattice, where the theory is made two-dimensional to account for the parallel inhomogeneities. No pre-assigned positions of the head groups, or other parts of the molecules, are introduced. Nearest neighbor interactions are accounted for through Flory-Huggins type interaction parameters. The theory is applied to the incorporation of trans-membrane molecules and conditions for channel formation are discussed. Lateral phase separation in membranes consisting of non-mixing lipids is also considered. Water only slightly enriches the boundary between the two lipid regions. The aliphatic chains are very well able to smoothly cover inhomogeneities in the bilayer. No indications of instability of the membrane due to the induced inhomogeneities are found.

Introduction

The structure of proteins in membranes is of great biological interest. Various statistical mechanical theories of lipid–protein interactions have been developed. Marčelja [1] modeled proteins as big rigid and structureless molecules which were surrounded by lipids arranging in two-dimensional hexagonal lattices and studied the ordering of the lipids around protein molecules. Similarly, Schröder [2] derived a differential equation to describe the change in order parameter when protein molecules are introduced into a lipid continuum. A more detailed microscopic model presented by Pink and co-workers [3,4] includes specific lipid–protein interactions that depend on the conformational state of the individual lipids. This model does not have molecular picture of the protein and requires many adjustable parameters. Scott and Coe [5] studied the effect of different lipid–protein interactions on the thermodynamic properties of the membrane. In this approach, the protein is again considered as essentially structureless.

In the model of Widom [6] the molecules are AA, AB, and BB dimers arranged on a two- or three-dimensional lattice so that only A ends or only B ends meet at any one lattice site. This is equivalent to an infinitely large repulsion between A and B segments. The molecules are self-assembling and the aggregates can have any shape. The addition of a bending energy enables the construction of phase diagrams of microemulsions. For the study of protein–lipid interactions in membranes this model is not sufficiently detailed.

More detailed information on the conformations of amphiphilic molecules in bilayers is obtained by self-consistent field (CSF) theories [7–10]. In most traditional models the head groups of the molecules are assumed to be fixed in parallel planes [7–9] and thus the establishment of thermodynamic equilibrium with the bulk solution is lost. Instead, it is usually assumed that water molecules are absent from the hydrophobic center of the bilayer and the membrane area per lipid molecule acts as a parameter which determines directly the bilayer thickness and indirectly the order parameters.

We introduced a more advanced self-consistent field lattice theory of lipid bilayer membranes [10–15]. In

Correspondence: J.M.H.M. Scheutjens, Laboratory for Physical and Colloid Chemistry, Wageningen Agricultural University, Dreijenplein 6, 6703 HB Wageningen, The Netherlands.

this theory the molecules are not attached to any plane or site. Also, we do not use any adjustable parameters. The structure of the bilayer is entirely determined by the solution properties of the molecules. Characteristics such as the area per molecule, the position of the head groups, the amount of water in the center of the bilayer, and bending energies are predicted by the model. In this theory Flory-Huggins type approach is used, i.e., combining Markov-type chain statistics with a local mean field approximation. All conformations are generated in a self-consistent potential field. The statistical weight per conformation is determined by using Boltzmann statistics, where the self-induced potential of mean force is a function of segment density profiles and Flory-Huggins interaction parameters. The membrane is stable due to the low water solubility of the apolar tails and the hydrophilic nature of the head groups. We use only three pair interaction parameters. The net repulsive interaction between apolar tail segments (A) and water (W), due to the hydrophobic effect, is responsible for the aggregation of the molecules. The net repulsion between head groups and tails leads to expulsion of head groups from the center of the membrane, and avoids a macroscopic phase separation. With these two parameters the assumption of a fixed position of the head groups is unnecessary. The third interaction parameter accounts for a net attraction between head groups and water (or, equivalently, a mutual repulsion between head groups). This parameter can only affect the details of the membrane structure. The effect of these parameters are shown in Refs. 12 and 13.

Molecular dynamics simulations and Monte Carlo methods are suitable for testing model predictions that cannot be verified experimentally. However, these computer experiments are very expensive and cannot reach equilibrium for complicated systems. Egberts and Berendsen [16] presented new molecular dynamics simulations on lipid bilayers and their results did not support the correlation between tail conformations found previously when the head groups were attached to (elastic) planes [17]. A simple version of our model [10] fits their data better than other available models. A detailed comparison between the SCF method and Monte Carlo simulation has been made by Wang and Rice [18]. An excellent agreement has been shown.

One strong point of our theory is that it can be used to examine a large variety of interfacial problems. We successfully modeled the polymorphism of surfactant micelles [11,15], investigated the entropy-energy balance in bilayer membranes composed of lecithin-like molecules [11,12], studied the free energy of curvature of the bilayer from lecithin vesicles [11,13], predicted the gel to liquid phase transition in lipid bilayer membranes [11,14]. In principle the theory can be used for microemulsions, surfactant adsorption, additives in membranes, etc, as well.

Flory-Huggins χ-parameters are used to describe the nearest neighbor interactions. These parameters have the advantage that they can be measured and tabulated. However, their value depends somewhat on the model used. Originally, only enthalpic interactions were accounted for in a χ-parameter. Entropic contributions like vibrations, rotations, etc. had to be modeled separately. It is now a common practice to consider χ-parameters as free energies which include a part of the mixing entropy. This makes it more difficult to calculate χ-values from the first principles, but it eliminates the need to explicitly model and evaluate these entropies. Other than temperature dependent, nonlinear entropy contributions such as the effects of free volume, excluded volume and long range interactions that are not properly accounted for in the Flory-Huggins approximation, can also affect the value of a χ-parameter. For quantitative predictions it is expedient to use a consistent set of χ-parameters, i.e., the same parameter values for the same class of models.

One of the drawbacks of the Flory-Huggins theory is that it does not take into account the local fluctuations in the concentration so that it applies best to concentrated solutions of (chain)molecules. In the self-consistent field theory this drawback is drastically reduced by allowing concentration gradients in one direction. We have shown that disallowing chain backfolding essentially affects the membrane thickness only by a constant factor [12]. This factor is around 1.4 if the number of segments per chain is kept constant, but as the number of segments per chain and hence their size should be rescaled in order to preserve the total flexibility of the chain, a more rigorous correction would probably reduce this factor to about unity.

In the theories presented so far all properties are averaged over lattice planes parallel to the membrane (mean field approximation). In the present paper, this restriction is relaxed, i.e., parallel inhomogeneities are now allowed and the incorporation of foreign substances like trans-membrane proteins can be mimicked. To achieve this, we develop a modified Markov approach for generating the conformations of the chain molecules. Segment density gradients are accounted for in two directions and a mean field approximation is applied in the remaining dimension.

To the authors' knowledge no rigorous statistical thermodynamical analyses of the complex membrane–protein interactions are available. Neither Monte Carlo nor molecular dynamic techniques can take into account the conformational freedom of both the protein and the lipid molecules at the same time. This is due to the extremely long computer time needed to solve the problem rigorously. At present only statistical mechanical techniques based on a self-consistent field are viable approaches to give information on these matters. In the following part we will discuss a first approach of a

theory designed for this goal. For clarity, the model will be presented in its simplest form for membranes in the fluid state. Although we do not yet take all specific interactions into account, the results give at least some semiquantitative insight into the subtle energy balances which are responsible for the high diversity of membrane systems. An additional feature is that the equilibrium conformation of the protein (modeled as a linear copolymer) is not pre-assigned but follows from the computations.

It is straightforward to incorporate the modifications that have been developed in papers [12–14] into the present model, based on Ref. 10. Nagle et al. [19] have suggested the introduction of Van der Waals attraction and other long range mean field interactions in lattice model. These interactions can simply be added to the nearest neighbor interactions. More essential for the present purpose is to incorporate parallel heterogeneities into our model, i.e., to change the theory from one-dimensional to two-dimensional.

An introduction into the model is given in Ref. 10. The next sections follow roughly the first part of Ref. 13 with slightly modified equations to allow for lateral concentration gradients. We give some typical results to illustrate the potentials of the model. Two examples of trans-membrane copolymer interactions are presented which demonstrate that the boundary layer of lipids between the membrane and the polymer molecules depends strongly on the strength of the interaction between the apolar segments of the copolymer and those of the lipid molecules. Under certain conditions the polymer can form a channel through the membrane. The last example shows a lateral phase separation in a two-component lipid bilayer. We think that the observed trends are realistic, even if quantitative predictions cannot be expected at the current state of the model.

Self-consistent field theory

A well-known theory to describe polymer solutions is due to Flory and Huggins (FH) [20]. This theory makes use of a lattice on which the polymer chain segments are placed using a first order Markov approximation. This means that a random walk approximation is applied in which the 'history' of the chain is only one step (segment) long. Backfolding to previously occupied lattice sites is allowed. Further, a mean field approximation over the whole homogeneous system volume is applied. The homogeneity in three dimensions is illustrated in Fig. 1a. With these approximations the partition function of a collection of chains on the lattice can be worked out analytically.

Scheutjens and Fleer (SF) extended the FH approach, and proposed a statistical mechanical model for homopolymer adsorption [21,22]. The SF approach makes use of modified Markov statistics in which inhomogeneities in one dimension (normal to the adsorbent surface) are allowed, while the mean field approximation in the other two dimensions is maintained. These

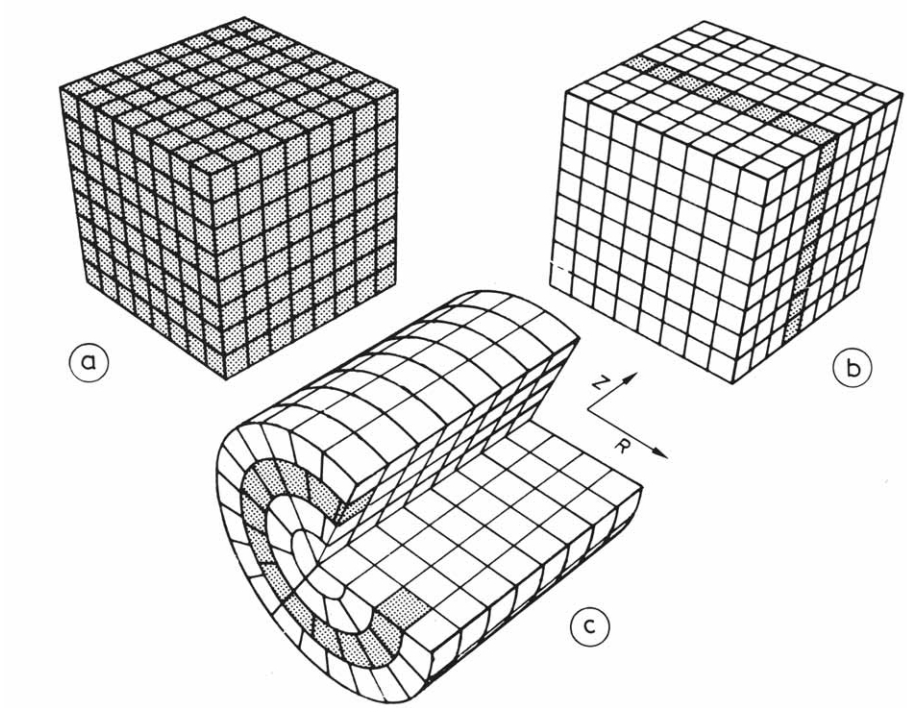

Fig. 1. Lattices used for: (a) FH theory, (b) SF theory, (c) 2D SF theory. The mean field approximation is applied over the whole space, within each lattice layer, and within each lattice ring, respectively.

two dimensions are sketched in Fig. 1b. Because segment density gradients in one direction are accounted for, the SF-theory may be called 'one-dimensional'. The partition function for these systems is available but can no longer be optimized analytically. Instead, the problem is reduced to a set of implicit equations which can be solved with standard numerical techniques. For adsorption from monomeric mixtures the theory reduces to the regular solution model of Ono and Kondo [23]. One of the advantages of this approach over Monte Carlo and molecular dynamics is that the computation times are only linearly proportional to the chain length of the polymer. Because of this low dependence of computation time on chain length, there are no problems to extend the theory to include an arbitrary number of different types of molecules. The theory has been extended to describe membrane systems [10].

Another advantage of the great computational efficiency is that a two-dimensional extension of the SF theory is feasible. To this end the lattice layers are divided into concentric equidistant rings. The rings in the various layers form cylinders and, for that reason, cylindrical co-ordinates are introduced. A similar Markov process is now applied in two directions, and the mean field approximation is applied only in each individual ring. In this way, the segment density gradients in the normal (z) and the radial (R) direction can be monitored. Thus the one-dimensional SF theory becomes two-dimensional. Fig. 1c shows a lattice representing the 2D modification of the SF theory. Concentric rings are drawn around a given point in successive flat planes. The flat layers are numbered $z = 1, \cdots, M_z$, where the z-direction is normal to the plane of the membrane, and the cylinders are numbered $R = 1, \cdots, M_R$, at layers $z = 1$, $z = M_z$, and $R = M_R$ reflecting boundaries are introduced. We note that M_z and M_R are preferably chosen so large that their precise positions are immaterial. In this way a virtually infinitely large system is simulated. In each layer z the number of lattice sites from the center up to ring number R is:

$$A(R) = \pi R^2 \tag{1}$$

The number of lattice sites is given by:

$$L(R) = A(R) - A(R-1) \tag{2}$$

The outer surface area of the ring with radius R is found by differentiation of Eqn. 1 with respect to R:

$$S(R) = 2\pi R \tag{3}$$

In this way, $S(R)$ is expressed in units of the face of a lattice site.

For the modified Markov-type statistics we need step probabilities for going from any given lattice site to any neighboring one. We allow steps down (to lower z), up, or in the same layer, and simultaneously we allow steps inward (to lower R), outwards, or in the same shell. We will make use of a hexagonal lattice with a coordination number $Z = 12$. (Z is assumed constant throughout the lattice.) The fraction of neighboring sites in the previous layer in the z direction is $\lambda_{-1}(z) = 1/4$ and that in the following layer is $\lambda_1(z) = 1/4$, leaving for the fraction of the neighboring sites in the same layer $\lambda_0(z) = 1/2$. These fractions can be considered a priori step probabilities, as they are solely defined by the geometry of the lattice and do not depend on the local interaction energies. For a step inwards or outwards the probabilities will depend on R. We choose these step probabilities proportional to the surface area of the face of the lattice site that is crossed if the step is made:

$$\begin{aligned} \lambda_{-1}(R) &= \frac{1}{4}\frac{S(R-1)}{L(R)} \\ \lambda_0(R) &= 1 - \lambda_{-1}(R) - \lambda_1(R) \\ \lambda_1(R) &= \frac{1}{4}\frac{S(R)}{L(R)} \end{aligned} \tag{4}$$

Now, a down-inward step will have a priori probability $\lambda_{-1,-1}(z, R) = \lambda_{-1}(z)\lambda_{-1}(R)$. Similar equations hold for the other eight step directions.

Special attention is required for defining the boundary conditions in the system. As far as the z-direction is concerned, reflecting boundaries have been introduced at layers $z = 1$ and $z = M_z$. This is realized by demanding identical behavior of layers $z = 0$ and $z = 1$ on the one side of the system, and similarly of layers $z = M_z$ and $z = M_z + 1$ on the other side of the system. For each chain leaving the system, i.e., across the boundary, we demand another chain from outside entering the system across the same boundary. A reflecting boundary introduces a symmetry-plane into the system. At the center $R = 0$ no lattice sites are available and the boundary is already specified by the step probabilities (no chains can leave the lattice at this side). However, the boundary between the cylinders M_R and $M_R + 1$ is less trivial. Again a reflecting boundary between two cylinders is assumed, i.e., $L(M_R + 1)$ and the a priori step probability for a step out of the system at this boundary is assumed to be the same as the a priori step probability into the system. We can expect errors caused by this idealized boundary when density gradients in the R direction are present near M_R. To minimize such artifacts, M_r is chosen so large that these inhomogeneities are negligible. Physically, this corresponds with the assumption that the lateral inhomogeneities are spatially remote from each other. In terms of the membrane–protein interaction, the proteins or the clusters in the membrane are very dilute and may not interact with each other.

Chain distributions in two dimensions

The chain molecules consist of segments with rank $s = 1, \cdots, r$. The segments are not necessarily identical. Although we will present results for branched lecithin-like molecules, we discuss for the sake of presentation only the distribution of linear chains in the present section. When the molecules are branched the statistics are somewhat more involved but this complications has already been worked out [11,12].

To find the distribution of the chain molecules, the statistical weight of each individual conformation must be known. A conformation of a molecule is defined by the sequence of coordinates (z, R) where the consecutive segments are situated. In general, each conformation is degenerate: various spatial configurations can have the same conformation.

A step-weighted random walk approximation is used for generating systematically all conformations of the chain molecules on the lattice. In the present approximation backfolding is allowed. The random walk approximation can be mathematically expressed in a recurrence relation which 'elongates' a chain of s segments into a chain of $s+1$ segments. Each elongation step from (z', R') to (z, R) in a random walk is weighted by its a priori step probability $\lambda_{z'-z,R'-R}(z, R)$, multiplied with a factor accounting for the potential of mean force experienced by the segments. This latter weighting factor (also called free segment weighting factor) is, for a given segment s, only a function of the position and type of the segment in the system: $G(z, R, s)$. When a segment is in a chain it possesses two bonds to neighboring segments. Bond 1 points towards a segment with lower rank and bond 2 points to a segment of higher rank. End segments have only one bond. The bonds of segment s are indicated by subscripts. For example, s_1' indicates that segment s' has only a bond of type 1, implying that it is an end segment. We define the chain end distribution function $G(z, R, s_1)$ as the weighting factor for segment s in position (z, R) subject to the requirement that bond 1 is connected to the remainder of the chain. With this chain end distribution function, the recurrence equation can be expressed as:

$$G(z, R, s_1) = G(z, R, s)\sum_{z'}\sum_{R'}\lambda_{z'-z,R'-R}(z, R)G(z', R', s_1') \quad (5)$$

In this equation bond 1 of segment s is connected to bond 2 of segment s'. Segment s is now the end of the chain. The recurrence relation is initiated at the first segment of the chain and, as $G(z, R, 1_1) = G(z, R, 1)$, only the free segment distribution functions and the a priori step probabilities need to be known to calculate all chain end distribution functions.

Scheutjens and Fleer [21] have shown that by combination with the complementary chain end distribution functions (the ones started at the other end of the chain, $G(z, R, s_2)$, obtained from Eqn. 5 by replacing subscripts 1 by subscripts 2) individual segment density profiles can be obtained from a composition formula which couples these two chain parts: one with s segments and the other with $r - s + 1$ segments:

$$\phi(z, R, s_{12}) = CG(z, R, s_{12})$$

$$= CG(z, R, s_1)G(z, R, s_2)/G(z, R, s) \quad (6)$$

Here, the division by $G(z, R, s)$ is introduced to correct for double counting of the overlapping segment and C is a normalization constant. For a given segment density ϕ^b of the molecules in the bulk solution $C = \phi^b/r$. Alternatively, when the total number of molecules $n = \Sigma_z\Sigma_R\Sigma_s L(R)\phi(z, R, s)$ in the system is known, $C = n/G(r_1)$, where $G(r_1) = \Sigma_z\Sigma_R L(R)G(z, R, r_1)$ is the total statistical weight of all chains in the system.

Free segment distribution functions have been derived before [11,12] and can be generalized to cover the present 2D analysis. They are Boltzmann factors containing the potential of mean force which depends on the local segment densities. A typical free segment distribution function depends on a hard core potential, $u'(z, R)$, independent of the segment type, and on interactions specific for a given segment type. When segment s is of type x then $G(z, R, s) = G_x(s, R)$, and

$$G_x(z, R) = \exp\left\{-\frac{u'(z, R)}{kT} - \sum_y \chi_{xy}\left(\langle\phi_y(z, R)\rangle - \phi_y^b\right)\right\} \quad (7)$$

Here, x and y represent the natures of the segments (for instance we represent the solvent by W, apolar segments by A, polar segments by B, etc.). The sum y is over all segment types. The quantity χ_{xy} is the well known Flory-Huggins interaction parameter which gives the pair energy difference in excess of the sum of those for the pure components. Therefore, only dissimilar contacts $(x \neq y)$ have a non-zero χ value. In the angular brackets in Eqn. 7, local averaging of the segment densities around a site at (z, R) is performed to obtain the appropriate average number of direct contacts:

$$\langle\phi(z, R)\rangle = \sum_{z'}\sum_{R'}\lambda_{z'-z,R'-R}(z, R)\phi(z', R') \quad (8)$$

The potentials of mean force $u'(z, R)$ in Eqn. 7 are originated from local hard core interactions ('excluded volume' or 'lateral pressure') and are introduced in the derivation as Lagrange multipliers. The reference state is the bulk solution, so that $u'^b = 0$. Similar quantities are introduced as $-kT \ln \alpha$ by Gruen [7] and as $-kT \ln q$ by Marqusee and Dill [8].

The set of Eqns. 5–7 cannot be solved analytically. To compute the segment density profiles (Eqn. 6) all

chain end distribution functions must be calculated (Eqn. 5). This is possible only when the free segment weighting factors (Eqn. 7) are known. These factors, in turn, depend on the segment density profiles (Eqn. 6) and $u'(z, R)$. Their values are found by numerical iteration, using the boundary condition that in each ring all lattice sites should be filled (packing constraint), i.e., $\Sigma_x \phi_x(z, R) = 1$ for all z and R. The total number of unknown variables $G_x(z, R)$ is equal to the total number of equations and boundary conditions. The set of implicit equations are solved by standard numerical methods [11,12].

It may be illustrative to express $u'(z, R)$ more explicitly. This is possible when a monomeric molecule, say water (W), is present. The volume fraction of W is obtained from Eqn. 6 as $\phi_w(z, R) = \phi_W^b G_W(z, R)$. In combination with Eqn. 7 we find directly $u'(z, R)/kT = -\ln(\phi_W(z, R)/\phi_W^b) - \chi_{AW}[\langle\phi_A(z, R)\rangle - \phi_A^b] - \chi_{BW}[\langle\phi_B(z, R)\rangle - \phi_B^b]$. If we now substitute the packing constraint $\phi_W(z, R) = 1 - \phi_A(z, R) - \phi_B(z, R)$, we see that the potential of mean force $u'(z, R)$ increases to infinity as $\phi_A(z, R) + \phi_B(z, R)$ approaches unity. This has the effect that this parameter controls the total density of molecules at (z, R). The final values of $u'(z, R)$ are usually a few tenths of a kT or less and can be positive as well as negative (with respect to the bulk solution).

The first-order Markov approach as discussed above is not very accurate for describing small chain molecules. For a better representation, a rotational isomeric state scheme which prevents the chain from direct backfolding can be applied [11,12]. However, the results are not affected qualitatively. When several segments of the chains are grouped in so-called statistical chain elements and the parameters are properly scaled, this problem is relaxed. In this paper, we choose the latter approach because much detail is irrelevant for the present purpose. The larger the segment size, the lower the resolution of the calculations. As a compromise, a statistical unit is chosen to be about three CH_2 segments long. Obviously, the energy parameters must be scaled to the segment size.

Reflecting boundaries

The reflecting (periodic) boundaries are realized by setting $G_x(z, r) = G_x(1 - z, R) = G_x(2M_z + 1 - z, R) = G(z, 2M_R + 1 - R)$ for all z and R. Membranes are generated near one of the boundary layers. As a consequence, membranes obtained in this way are symmetrical with respect to their midplane. In addition to reducing computation time (only half of the membrane has to be calculated) this boundary condition is also used to fix the lattice on the membrane. Translational freedom of the membrane in the system is disregarded because it is irrelevant for the present issue. Similarly, the lateral inhomogeneities are restricted to a region around the center of the lattice (near $R = 1$). Consequently, the translational entropy, originating from the distribution of the inhomogeneities along the bilayer is neglected. When necessary, such entropy terms can be included [11,15].

Results and Discussion

Basic membrane structure

To start the analysis we first describe the segment density profiles of a membrane composed of lecithin molecules. For a lecithin molecule, the following architecture is chosen:

$$\begin{array}{l} A_p - B - A \\ \qquad\quad | \\ A_p - B - A \\ \qquad\quad | \\ \qquad\quad A - B_q \end{array} \qquad (9)$$

Here, p is the number of statistical units (each 3 CH_2 units long) of apolar tail segments A, and q is the number of polar head group units B. Near the glycerol backbone the statistical units are a little unrealistic. Also, we will neither model any details in the head group itself, nor account for the larger volume of the CH_3 end groups as compared with the CH_2 groups of the chain. The solvent (W) is modeled as monomers which are clusters of water as big as the (statistical) units of the chain molecules. The Flory-Huggins parameters are chosen to mimic a lecithin (with tails of 16 CH_2 segments), for which the RIS-scheme calculations have been worked out before [11,12]. The net interaction between $(CH_2)_3$ and (clusters of) water is about $\chi_{AW} = 3$, in accordance with the solubility data given by Tanford [24], whereas $\chi_{BW} = -0.5$ and $\chi_{AB} = 2.7$. The value of χ_{AW} should be high enough to induce aggregation of the lecithin molecules and determines the equilibrium concentration of these molecules in the solution and the amount of water in the center of the membrane. The calculations are not very sensitive to χ_{BW}. The actual value of χ_{BW} depends on the type of head group segments, but must be negative because the net interaction with water is attractive. The interaction between head groups and tails is not considered in most theories. In the present model the position of the head groups is not fixed but a positive high value for χ_{AB} will tend to push the head groups out of the center of the membrane. The solubility of head-group segments in the apolar center of the membrane is assumed to be slightly better than that of water ($\chi_{AB} < \chi_{AW}$), but no experimental data are available. The effects of the interaction parameters have been shown in Refs. 12 and 13.

Fig. 2 shows the segment density profiles of an equilibrium membrane (i.e., with a vanishing surface

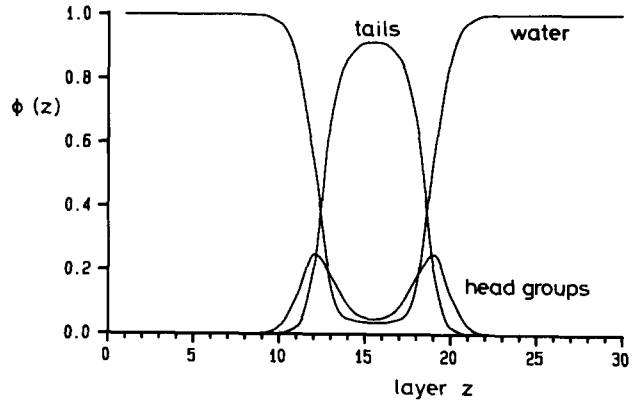

Fig. 2. Segment density profiles through a cross section of a membrane composed of lecithin molecules ($p = 6$, $q = 2$). The equilibrium concentration is $1.6 \cdot 10^{-8}$, and the excess free energy is zero. The energy parameters are $\chi_{AW} = 3$, $\chi_{BW} = -0.5$ and $\chi_{AB} = 2.8$, where A is an apolar segment, B a polar segment, and W represents solvent molecules.

tension) consisting of lecithin molecules ($p = 6$ and $q = 2$). In this case there are no lateral inhomogenities and, consequently, the results are exactly the same as in the one-dimensional model. The very unfavorable tail-water contacts cause the center of the membrane to be almost devoid of water. Further, the segment density profiles show rather broad distributions indicating that the chains do have a considerable amount of conformational entropy. The equilibrium value fraction of lipids in the bulk solution is $1.6 \cdot 10^{-8}$. In the following calculations, where additives are introduced into the system, the amount of lipids is chosen so that this equilibrium concentration is essentially identical.

Trans-membrane configuration of a copolymer molecule in the bilayer

The copolymer guest molecule is modeled by a chain with apolar A′ and polar B′ segments. The prime denotes that the segment belongs to the copolymer. As we want to investigate the effect of the apolar segments of the guest molecule and that of the lipid, we allow the nature of segment A′ to differ from that of A. Like B, the polar segments B′ are water soluble but, if desired, we can introduce some repulsion or attraction between B′ and B. We have chosen a linear symmetrical copolymer molecule. For such a molecule the two ends have mirror sequences of polar and apolar segments. Since the present calculations are only for illustrating a trans-membrane configuration, we refrained from an exhaustive analysis and choose arbitrarily the following specific copolymer which has 200 units of which 72 are polar:

$$(B'_6 - A'_8 - B'_6 - A'_{16} - B'_6 - A'_{16} - B'_6 - A'_{16} - B'_6 - A'_8 - B'_6)_2 \qquad (10)$$

Fig. 3 shows the segment density profiles of this polymer molecule in a homogeneous solution. These segment density profiles are two-dimensional. The layers and rings are renumbered in such a way that the center of the lattice is not at $(z, R) = (0.5, 0.5)$ but at (10.5, 10.5). To minimize the number of apolar-water contacts, the molecule assumes a collapsed configuration. As one can see the configuration is globular. Note that in our approach the molecule is not forced into a globular structure. It could for example have chosen a rod-like configuration and, in fact, molecules of other composition might prefer that.

In Fig. 4 copolymer molecules are introduced into the membrane. Clearly, the chain molecule has re-

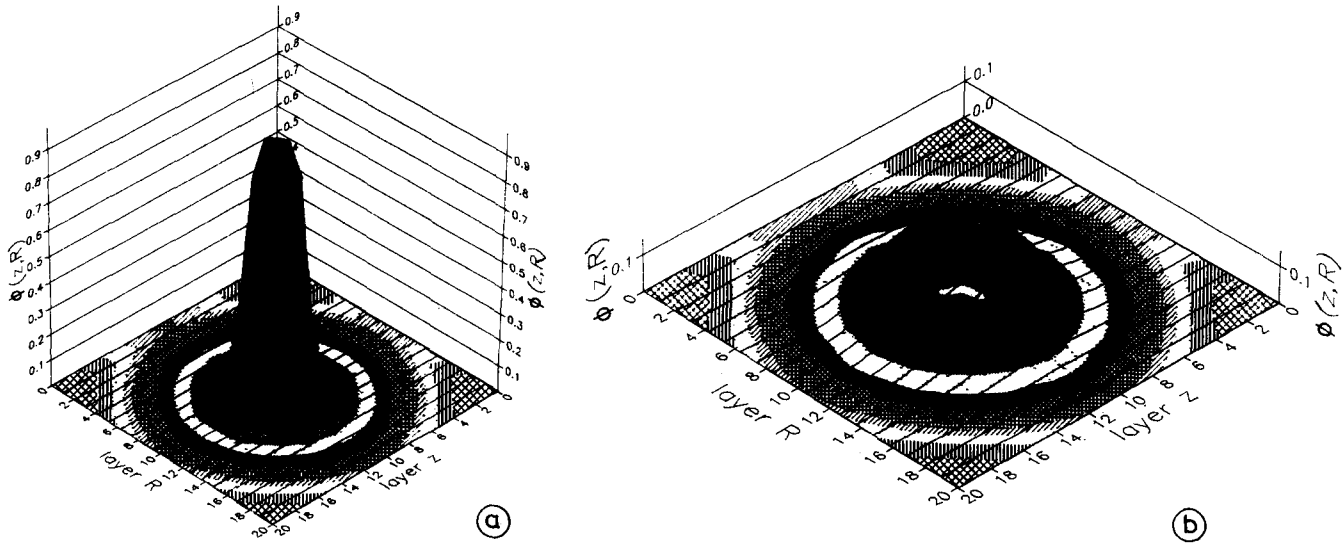

Fig. 3. Segment density profiles through a cross section of the copolymer given in Eqn. 10 in pure solvent. The R and z axes are shifted so that the centre of the copolymer is at (10.5, 10.5). The energy parameters are $\chi_{A'W} = 2.7$, $\chi_{B'W} = 0.5$, $\chi_{A'B'} = 2.8$. (a) Apolar segments A′. (b) Polar segments B′.

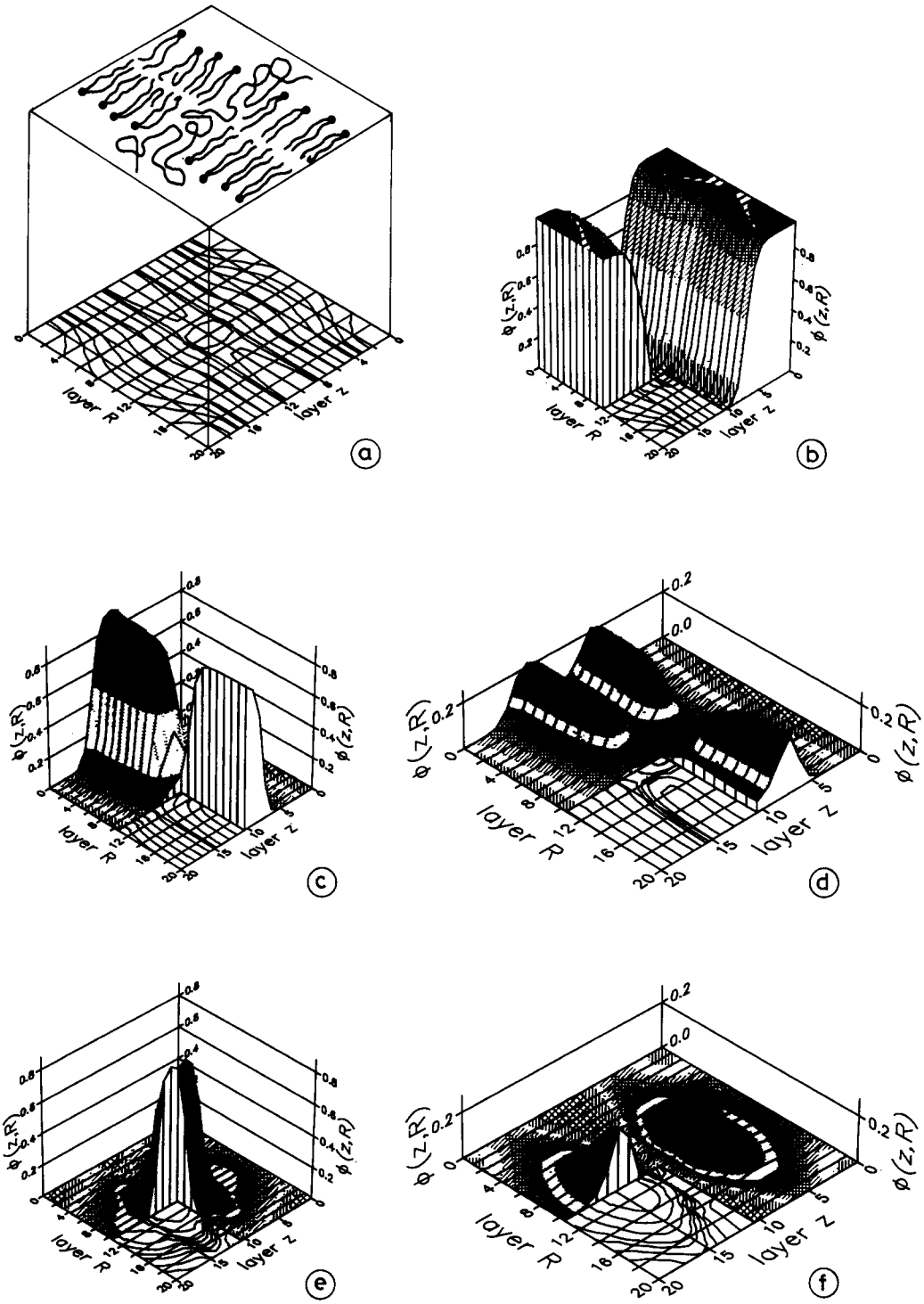

Fig. 4. Two-dimensional segment density profiles of the membrane given in Fig. 2 in interaction with the guest molecule given in Fig. 3. Additional energy parameters: $\chi_{AA'} = 0.8$, $\chi_{BB'} = 0$, $\chi_{AB'} = \chi_{BA'} = 2.8$; other parameters as in Fig. 2. The copolymer molecule is put in the center of the lattice. The lattice layers are numbered arbitrarily. Where expedient, one quarter of the figure is cut out of the profiles to show details to the behavior in the center. For this quarter the iso-ϕ_W lines are plotted. (a) Upper plane: artist's view. Lower plane: iso-ϕ_W lines. (b) Solvent density profiles. (c) Apolar segments of the lipid molecules. (d) Polar segments of the lipid molecules. (e) Apolar segments of the copolymer molecule. (f) Polar segments of the copolymer molecule.

arranged its segments with the tendency to have polar moieties located at the outside of each side of the membrane. At the boundaries of the system, i.e., near $R = 0$ and $R = 20$, the membrane has its unperturbed shape. Near the lattice center the segment profiles of the membrane are perturbed. However, even at the mid-

point, where the segment density of the guest molecule is very high, some lipid tails are present.

In the present example, most of the corresponding energetic interactions of the polar and apolar segments of the two types of molecules are chosen identical. The most sensitive parameter for the distribution is the interaction between the apolar tails of the lipid molecules and the apolar segments of the copolymer. To obtain a compact segment density of the copolymer in the heart of the membrane, this interaction must be repulsive. In the present case $\chi_{AA'} = 0.8$. Since the guest molecule is not of extremely high molecular weight, the profiles of the copolymer and the lipid tails do overlap. Reducing the value for $\chi_{AA'}$ would increase this overlap and eventually the copolymer would dissolve in the center of the membrane to form a more or less 'random' coil. A much higher value for $\chi_{AA'}$ would increase the separation between the two types of apolar segments. We also generated (not shown) this latter type of membrane-copolymer structures and found that they exist only when the membrane was short of lipids per surface area (i.e., the membrane is not in full equilibrium). In this case more lipids were offered to the bilayer and the copolymer was pushed out of the membrane. This indicates that very large deviations in membrane properties cannot exist in the boundary layers as long as the membrane is in equilibrium.

Other parameters can also be relevant for the incorporation of a copolymer in the membrane. The polar–apolar χ_{AB}, $\chi_{A'B}$, $\chi_{AB'}$, and $\chi_{A'B'}$ interactions, inherent in the problem because of the architecture of the amphiphilic molecules, can shift the position of the central molecule when variations in the interactions are introduced.

Cluster of four trans-membrane copolymer molecules in the bilayer

As a second example of membrane–copolymer interaction, we incorporated a more polar chain molecule of the same length, with 104 B′ segments and the following arbitrary segment sequence:

$$(B'_{10} - A'_4 - B'_6 - A'_{10} - B'_5 - A'_5 - B'_5 - A'_{10} - B'_5 - A'_5 - B'_5 - A'_{10} - B'_6 - A'_4 - B'_{10})_2 \quad (11)$$

In Fig. 5 the segment density profiles of a free molecule are indicated. In comparison with Fig. 3 one can see that this molecule is more hydrophilic: it has more polar parts and does not have long apolar parts. Also in this case the structure is almost globular. Due to its longer polar parts this copolymer molecule has segment profiles that are significantly different from those shown in Fig. 3.

Since this molecule is much more polar, we cannot expect the copolymer to incorporate into the membrane as easily as in our previous example. Adsorption of the copolymer onto the membrane is more likely. As our membranes are symmetrical, adsorption on the membrane surface occurs at both sides simultaneously and, consequently, at least two copolymer molecules are involved. If the chain molecules on the two sides push some head groups of the lipids apart, it would be rather difficult, if not impossible, for the lipids to fill up the space between the sandwich formed by the two copo-

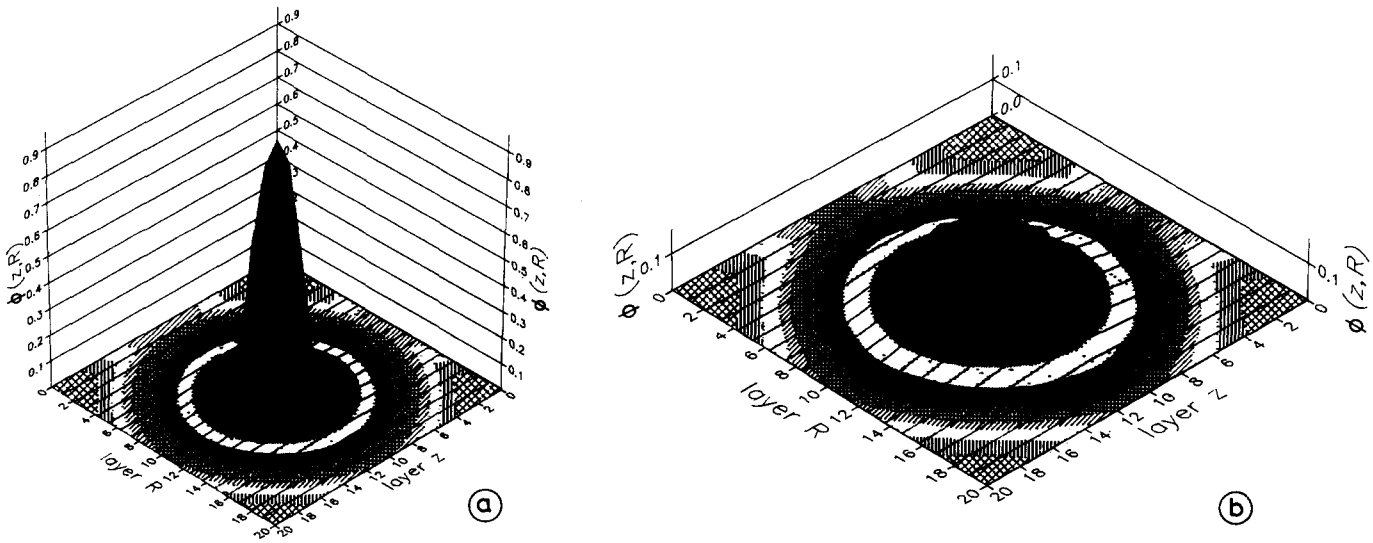

Fig. 5. Segment density profiles through a cross section of the copolymer given in Eqn. 11 in pure solvent. Energy parameters as in Fig. 3. (a) Apolar segments. (b) Polar segments.

lymers. This explains why we were also unable to find in this case a thermodynamically stable situation with two copolymer molecules in the membrane. Surprisingly, we observed a very remarkable equilibrium structure when four such copolymer molecules were put together in the lipid membrane. Fig. 6 gives the segment distribution for this situation, which could not be obtained with the more apolar copolymer. As can be seen, a cluster of four molecules did arrange themselves in the lipid membrane, with a clear channel in the center. This observation may be the root of an explanation of the spontaneous formation of pores, allowing cross-membrane transport. Of course, we do not claim that this structure is the only (thermodynamically) stable one.

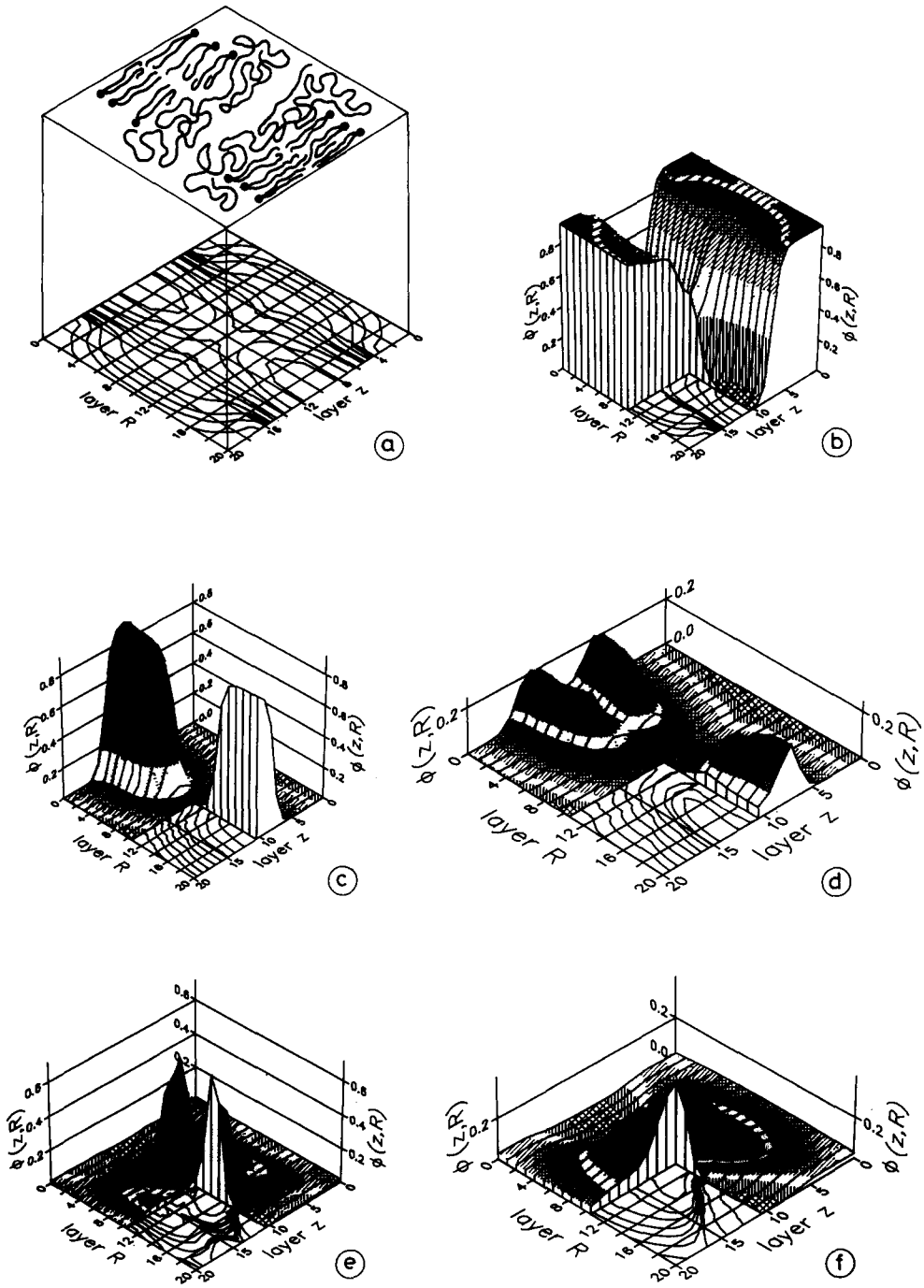

Fig. 6. Two-dimensional segment density profiles of the membrane given in Fig. 2 in interaction with four copolymers as given in Eqn. 11. The additional interaction parameters are: $\chi_{AA'} = 0.7$, $\chi_{BB'} = 0.5$, and $\chi_{AB'} = \chi_{A'B} = 2.8$. (a) Upper plane: artist's view. Lower plane: iso-ϕ_W lines. (b) Solvent density profiles. (c) Apolar segments of the lipid molecules. (d) Polar segments of the lipid molecules. (e) Apolar segments of the four copolymer molecules. (f) Polar segments of the four copolymer molecules.

For instance, clusters with three or five copolymer molecules could have been more favorable but we have not investigated such possibilities systematically. As in our first example, we have introduced a repulsion between the apolar segments of the copolymer and the lipid tails: $\chi_{AA'} = 0.7$. We also assumed a repulsion between the two types of polar segments: $\chi_{BB'} = 0.5$. This repulsion did also contribute to the partitioning between the polar segments of the lipid head groups and the probe. When the apolar segments mix better, the four copolymers would feel even better at their present position. The hydrophilic heart of the aggregate shows that 'proteins' can spontaneously form hydrophilic pores through which the transport of polar molecules may occur.

In many experimental studies on membrane protein interactions, high protein/lipid ratios are encountered. Our second example may be relevant for these studies.

Lateral phase separation

Fig. 7 shows the segment density profiles of a homogeneous membrane composed of lecithin molecules of $p' = 7$ apolar and $q' = 3$ polar segments. For this membrane the excess free energy (and hence the surface tension) is zero and the equilibrium lipid volume fraction in the solution is: $8.6 \cdot 10^{-10}$. As compared with the segment density profiles given in Fig. 2, this membrane is slightly thicker because the apolar tails of the lipids are one unit longer. Therefore, the equilibrium volume fraction in the solution is lower.

Fig. 8 shows the two-dimensional segment density profiles of the two molecules ($p' = 7$, $q' = 3$ mixed with $p = 6$, $q = 2$) in one system. In this case $(z, R) =$ (10.5, 14.5) is the center of the lattice. We assigned a repulsion between the two types of apolar segments: $\chi_{AA'} = 0.5$ and a stronger repulsion between segments of the two types of head groups: $\chi_{BB'} = 1$. These repulsions cause a lateral phase separation. Studying the segment density profiles reveals that in the boundary area the concentration of solvent is slightly higher than in either of the two homogeneous membrane phases. This is caused by the fact that the two molecules avoid each other, and thus the water molecules enter to fill the space. High solvent concentrations are, however, not found in the interfacial region between the two lipids. The energetic effect of exposing tails to water is so unfavorable that the tails fill up most of the space. Very extreme situations are needed to find an interfacial region in which the water concentration is high. There are no indications of membrane rupture.

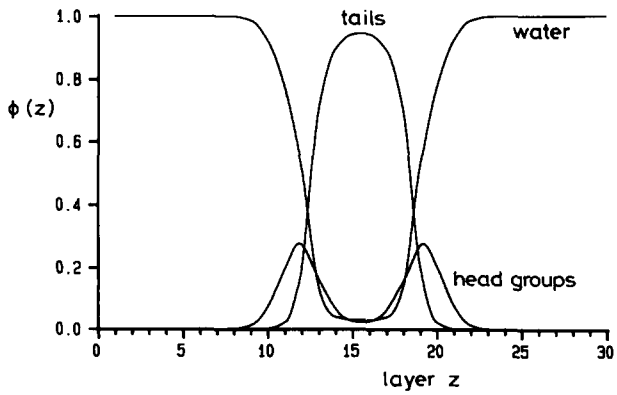

Fig. 7. Segment density profiles of a cross section through a homogeneous membrane composed of lecithin molecules with $p' = 7$ and $q' = 3$. Interaction parameters as in Fig. 2.

Conclusions

We have extended our Self-Consistent Field theory of associated amphiphilic molecules to include inhomogeneities in two directions. The potentials of the model are demonstrated by applying it to the incorporation of guest molecules into lecithin membranes. Two examples of membrane–copolymer interactions are discussed, a trans-membrane copolymer and a cluster of four polymers in the lipid membrane. In the latter the four molecules associated to form a channel, through which transport of hydrophilic molecules is possible. In the membranes, the conformations of these copolymers differed dramatically from those in an aqueous solution.

We also studied lateral phase separation in membranes consisting of two different lipids. The boundary layer between the two lipid phases was found to be as hydrophobic as in either phase.

The present theory is specifically useful for systems which are characterized by inhomogeneities in interfaces such as: adsorption of chain molecules on heterogeneous surfaces, surfactant adsorption (formation of hemimicelles), reverse micelles in membranes, etc. It is possible to improve the present theory in various respects. One could think of correcting for backfolding by incorporating the rotational isomeric state scheme [11,12] and accounting for an anisotropic orientational molecular field [11,14] to improve on modeling the excluded volume of the other chains.

In the present model a cylindrical symmetry is imposed on the concentration profiles. This may be a poor approximation for proteins in a membrane. It is possible to relax this restriction somewhat by replacing the circular lattice rings by elliptical rings, similar to the approach described in Refs. 15 and 25, and check whether such an elliptical symmetry has a lower free energy.

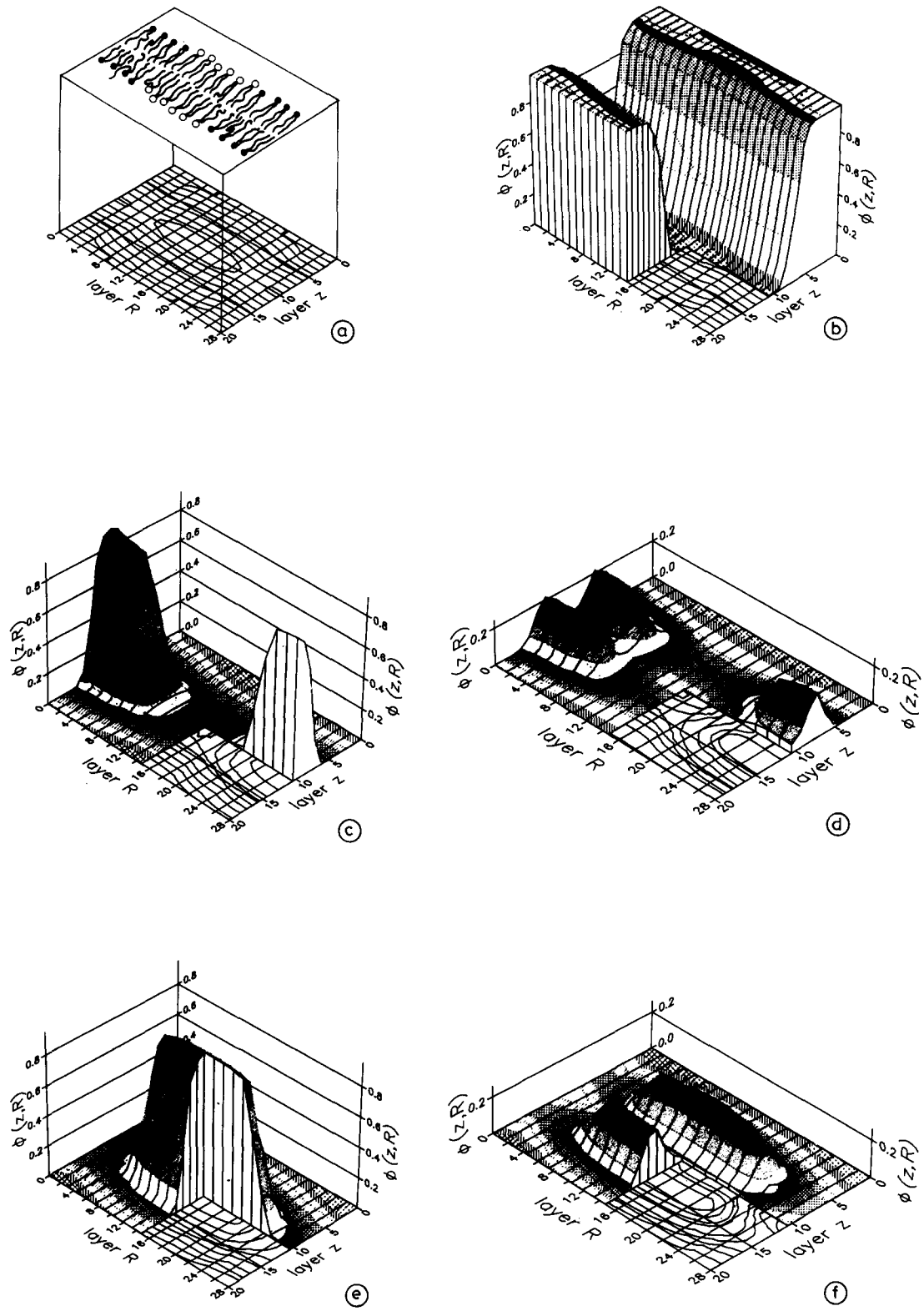

Fig. 8. Two-dimensional segment density profiles of two nonmixing types of lipid molecules given in Fig. 2 ($p = 6$, $q = 2$) and Fig. 7 ($p' = 7$, $q' = 3$). The additional energy parameters are: $\chi_{AA'} = 0.5$ and $\chi_{BB'} = 1$. (a) Upper plane: artist's view. Lower plane: iso-ϕ_W lines. (b) Solvent density profiles. (c) Apolar segments $p = 6$. (d) Polar segments $q = 2$. (e) Apolar segments $p' = 7$. (f) Polar segments $q' = 3$.

Acknowledgements

The work of F.A.M.L. is part of the research programme of the Stichting Scheikundig Onderzoek Nederland (SON), which is financially supported by the Nederlandse Organisatie voor Wetenschappelijk Onderzoek (NWO).

References

1 Marčelja, S. (1976) Biochim. Biophys. Acta, 455, 1–7.
2 Schröder, H. (1977) J. Chem. Phys. 67, 1617–1619.
3 Pink, D. and Chapman, D. (1979) Proc. Natl. Acad. Sci. USA 76, 1542–1546.
4 Tessier-Lavigne, M., Boothroyd, A., Zuckermann, M.J. and Pink, D.A. (1982) J. Chem. Phys. 76, 4587–4599.
5 Scott, H.L., Jr. and Coe, T.J. (1983) Biophys. J. 42, 219–224.
6 Widom, B. (1986) J. Chem. Phys. 84, 6943–6954.
7 Gruen, D.W.R. (1985) J. Phys. Chem. 89, 146–153.
8 Marqusee, J.A. and Dill, K.A. (1986) J. Chem. Phys. 85, 434–444.
9 Szleifer, I., Ben-Shaul, A. and Gelbart, W.M. (1987) J. Chem. Phys. 86, 7094–7108.
10 Leermakers, F.A.M., Scheutjens, J.M.H.M. and Lyklema, J. (1983) Biophys. Chem. 18, 353–360.
11 Leermakers, F.A.M. (1988) PhD thesis, Wageningen Agricultural University.
12 Leermakers, F.A.M. and Scheutjens, J.M.H.M. (1988) J. Chem. Phys. 89, 3264–3274.
13 Leermakers, F.A.M. and Scheutjens, J.M.H.M. (1989) J. Phys. Chem. 93, 7417–7426.
14 Leermakers, F.A.M. and Scheutjens, J.M.H.M. (1988) J. Chem. Phys. 89, 6912–6924.
15 Leermakers, F.A.M., Van der Schoot, P.P.A.M., Scheutjens, J.M.H.M. and Lyklema, J. (1988) in Surfactants in Solutions. Modern Applications (Mittal, K.L., ed.), in press.
16 Egberts, E. and Berendsen, H.J.C. (1988) J. Chem. Phys. 89, 3718–3732.
17 Van der Ploeg, P. and Berendsen, H.J.C. (1982) J. Chem. Phys. 76, 3271–3276.
18 Wang, Z.-G. and Rice, S.A. (1988) J. Chem. Phys. 88, 1290–1297.
19 Nagle, J.F., Gujrati, P.D. and Goldstein, M. (1984) J. Phys. Chem. 88, 4599–4608.
20 Flory, P.J. (1953) Principles of Polymer Chemistry, Cornell University Press, Ithaca NY.
21 Scheutjens, J.M.H.M. and Fleer, G.J. (1979) J. Phys. Chem. 83, 1619–1635.
22 Scheutjens, J.M.H.M. and Fleer, G.J. (1980) J. Phys. Chem. 84, 178–190.
23 Ono, S. and Kondo, S. (1960) in Handbuch der Physik (Flügge, S., ed.), Vol. 10, pp. 262–280, Springer, Berlin.
24 Tanford, C. (1973) The Hydrophobic Effect: formation of micelles and biological membranes, John Wiley, New York.
25 Leermakers, F.A.M. and Scheutjens, J.M.H.M. (1990) J. Colloid Interface Science, in press.